

Wigner crystallization in  $\text{Na}_3\text{Cu}_2\text{O}_4$  and  $\text{Na}_8\text{Cu}_5\text{O}_{10}$  chain compoundsP. Horsch, M. S. Son, M. M. Mayr, and M. Jansen<sup>1</sup><sup>1</sup>Max-Planck-Institut für Festkörperforschung, Heisenbergstrasse 1, D-70569 Stuttgart, Germany  
(Dated: March 22, 2024)

We report the synthesis of novel edge-sharing chain systems  $\text{Na}_3\text{Cu}_2\text{O}_4$  and  $\text{Na}_8\text{Cu}_5\text{O}_{10}$ , which form insulating states with commensurate charge order. We identify these systems as one-dimensional Wigner lattices, where the charge order is determined by long-range Coulomb interaction and the number of holes in the d-shell of Cu. Our interpretation is supported by X-ray structure data as well as by an analysis of magnetic susceptibility and specific heat data. Remarkably, due to large second neighbor Cu-Cu hopping, these systems allow for a distinction between the (classical) Wigner lattice and the  $4k_F$  charge-density wave of quantum mechanical origin.

PACS numbers: 71.10.-w, 71.28.+d, 75.10.Pq

The role of strong electron correlations and the concomitant appearance of spatially modulated charge structures constitutes a central issue in current solid state physics [1]. The most prominent example are charge stripes in high- $T_c$  superconductors, which have been discovered first as static modulations in the  $\text{CuO}_2$  planes of  $\text{La}_{1.6-x}\text{Nd}_{0.4}\text{Sr}_x\text{CuO}_4$  [2]. The high- $T_c$  enigma has at the same time stimulated the flourishing field of low-dimensional cuprates composed of Cu-O chains and ladders [3] with the hope to gain new insights overlooked so far in the layered cuprates. One important aspect is the role of long-range Coulomb interaction in strongly correlated systems, which gives rise to metal/insulator stripe structures in organic charge-transfer compounds [4].

Following a recently discovered new route in the synthesis of alkali oxometallates [5], we were able to synthesize several members of a new class of quasi-1D cuprates  $\text{Na}_{1+x}\text{CuO}_2$ . These intrinsically doped edge-sharing chain systems provide a unique opportunity to study the condensation of charge order (CO) at high temperature and the formation of spatially modulated Heisenberg spin systems at low temperature. Edge-sharing chains are also building blocks of the intensively studied  $\text{Sr}_{1.4-x}\text{Ca}_x\text{Cu}_2\text{O}_{41}$  system; due to exchange of electrons with ladders, however, the degree of doping is difficult to determine [6]. Here, we argue that these doped chains can be understood as realizations of one-dimensional Wigner lattices (WL) [7], as introduced by Hubbard [8] in the late 70's in connection with TCNQ charge transfer salts. He suggested that the distribution of electrons is controlled by the Coulomb interaction rather than by the kinetic energy (band width), such that they form a generalized Wigner lattice on the underlying TCNQ chain structure. This view suggests a strikingly different nature of charge excitations, namely as domain walls with fractional charge rather than particle-hole excitations as in common metals and semiconductors. Hubbard's proposal, however, can be challenged on the grounds that the resulting periodicity of charge modulation can alternatively be explained by a  $4k_F$  charge density wave (CDW) [9, 10, 11] arising from short-range

interactions alone and an instability of the Fermi surface, where  $k_F$  denotes the Fermi momentum.

The edge-sharing arrangement of  $\text{CuO}_4$  squares meets the WL criterion of small band width in an optimal way due to the almost  $90^\circ$  Cu-O-Cu bonds (Fig. 1). Unexpected complexity is added because, apart from a small nearest-neighbor hopping matrix element  $t_1$ , there is also a second neighbor hopping  $t_2$ , which is larger as a consequence of the structure. While this unusual feature does not affect the classical WL order imposed by the Coulomb interaction, it changes the Fermi surface topology, and thereby allows to distinguish the WL from the CDW on the basis of the modulation period.

These systems provide a first example where an unambiguous distinction between the generalized WL and a Fermi surface related  $4k_F$  CDW is possible. We also show that for these edge-sharing compounds even the magnetic and thermodynamic properties can only be explained by invoking a WL ground state emerging from the truly long-ranged Coulomb interaction.

Samples were prepared by the azide/nitrate route [5]. As a source for the alkaline metal component, mixtures of the respective alkali azides and nitrates (or nitrites) are used instead of the alkali oxides. Conveniently, besides the metals' ratio, also the oxygen content and thus the degree and kind of doping of the desired product can be effectively controlled using the weighed portions of the starting materials. Following this procedure the title compounds  $\text{Na}_3\text{Cu}_2\text{O}_4$  ( $x = 1=2$ ) and  $\text{Na}_8\text{Cu}_5\text{O}_{10}$  ( $x = 3=5$ ) have been prepared as microcrystalline, pure phases in gram amounts. The new oxocuprates (II/III) belong to the compositional series  $\text{Na}_{1+x}\text{CuO}_2$ , with the end members  $\text{NaCuO}_2$  [12] and the still elusive  $\text{Na}_2\text{CuO}_2$ . The most prominent structural feature, common to all representatives known thus far, is a one-dimensional polyanion  $\text{CuO}_2^n$  constituted of  $\text{CuO}_4$ -square units sharing edges in transposition. These anionic entities are embedded by sodium ions which achieve coordination numbers of 4-6 with Na-O bond lengths ranging from 227 to 279 pm. The geometric data as determined by single crystal structural analyses give clear evidence for a

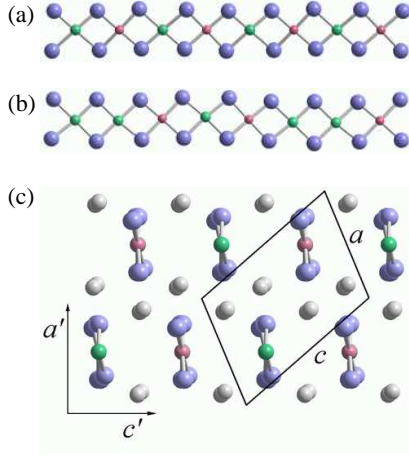


FIG. 1: Structure of edge-sharing copper-oxygen chains along  $b$ -direction in  $\text{Na}_3\text{Cu}_2\text{O}_4$  (a) and  $\text{Na}_8\text{Cu}_5\text{O}_{10}$  (b), where  $\text{Cu}^{2+}$  and  $\text{Cu}^{3+}$  are marked by green and red circles, and  $\text{O}^{2-}$  ( $\text{Na}^+$ ) by large blue (grey) circles, respectively. (c) View on the  $a$ - $c$  plane of  $\text{Na}_3\text{Cu}_2\text{O}_4$ . For convenience we introduce a cartesian system  $a'$ ,  $b'$ ,  $c'$  in addition to crystallographic coordinates.

CO at the Cu sites (Fig. 1). Based on the Cu to O bond lengths, one can unambiguously distinguish  $\text{Cu}^{3+}$  and  $\text{Cu}^{2+}$  sites. The way of linking the primary structural units together with the variations of the copper to oxygen distances inevitably leads to deviations of the O-Cu-O angles from the ideal  $90^\circ$ . As monitored by differential scanning calorimetry measurements CO disappears above the WL melting temperature  $T_m = 455$  and  $540$  K for  $\text{Na}_3\text{Cu}_2\text{O}_4$  and  $\text{Na}_8\text{Cu}_5\text{O}_{10}$ , respectively. DC and AC conductivity measurements show also a clear transition from an Arrhenius behaviour below  $T_m$  to an almost temperature independent conductivity regime above  $T_m$ .

For a theoretical analysis one has to recognize that  $\text{Cu}^{2+}$  is in a  $d^9$  configuration with spin  $1/2$ , while  $\text{Cu}^{3+}$  is in a  $d^9$ -ligand hole ( $d^9 L_h$ ) state, also known as Zhang-Rice singlet state [13]. In contrast to high- $T_c$  cuprates the edge-sharing geometry (Fig. 1(a,b)) leads to strongly reduced hopping matrix elements. This sets the stage for the long-range Coulomb force as dominant interaction

$$H_{\text{Coul}} = U \sum_i n_{i\uparrow} n_{i\downarrow} + \sum_{i,j \neq i} V_{ij} n_{i\uparrow} n_{j\uparrow}; \quad (1)$$

where the on-site interaction  $U$  suppresses charge fluctuations involving  $\text{Cu}^{1+}$  ( $d^{10}$ ) configurations. Here we associate the  $d^9 L_h$  ( $d^9 d^{10}$ ) ionization state with 0 (1,2) electrons, respectively, and  $n_{i\sigma}$  ( $\sigma = \uparrow, \downarrow$ ) counts the number of electrons with spin  $\sigma$ , while  $n_i = n_{i\uparrow} + n_{i\downarrow}$ . The Coulomb interaction  $V_1$  in general is screened by the polarization of neighbouring chains as well as by core electrons [8]. Here we assume a generic Coulomb law  $V_l = \frac{V_1}{l}$ ,  $l = 1, 2, \dots$  [14]. Crucial for the following is that the interaction is long ranged and convex, i.e.,  $V_1^0 = V_{1-1} - 2V_1 + V_{1+1} > 0$ .

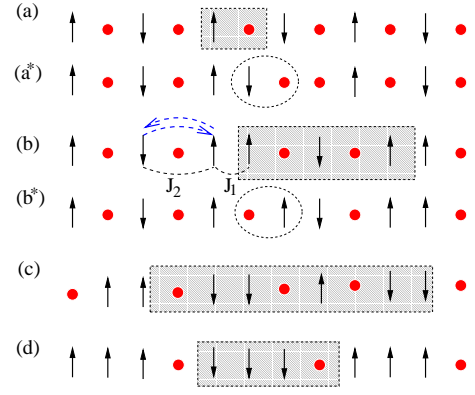


FIG. 2: (color online) Wigner charge order resulting from Coulomb repulsion and associated modulated Heisenberg spin structure for  $x = 1/2, 3/5, 5/8$  and  $3/4$  doping (a-d). The spin- $1/2$  of  $\text{Cu}^{2+}$  (arrows) is responsible for magnetism;  $\text{Cu}^{3+}$  (circles) is nonmagnetic. The spin arrangement is that expected for ferromagnetic exchange  $J_1$  and antiferromagnetic  $J_2$ , where the two excitations  $d^9 d^9 \rightarrow d^9 L_h d^{10}$  contributing to  $J_2$  are indicated by dashed arrows in (b). The charge unit cells (shaded) contain 2, 5, 8, 4 sites, respectively. The structures (a) and (b) are realized in  $\text{Na}_3\text{Cu}_2\text{O}_4$  and  $\text{Na}_8\text{Cu}_5\text{O}_{10}$ , respectively, and the dashed circles in (a) and (b) indicate charge excitations / V in these structures. (d) Typical modulation for charge stripes in cuprates at doping  $1/8$ .

For commensurate doping concentration  $x = m/n$  the interaction  $V_1$  selects a particular CO pattern [8]. This pattern is immediately obvious for filling fractions  $x = 1/2$  and  $3/4$  (Fig. 2(a,d)) which involve an equidistant arrangement of the  $\text{Cu}^{3+}$  sites (red circles in Fig. 2). For a general ratio  $x = m/n$  this leads to complex structures with unit cell size  $n$  (in units of the Cu-Cu distance  $b^0 = 1$ ). In case of  $x = 3/5$  we encounter in Fig. 2(b) the charge order observed for  $\text{Na}_8\text{Cu}_5\text{O}_{10}$ . Charge localization, however, is not perfect in Wigner insulators as electrons still undergo virtual transitions to neighboring sites (Fig. 2(a,b)) in order to retain partially their kinetic energy. The energy of the lowest excitations and the impact of kinetic energy depend strongly on  $x$ , e.g., the energy of the excitation in Fig. 2(a) relative to the ground state Fig. 2(a) is  $V_2^0$  while the excitation for  $x = 3/5$  in Fig. 2(b) is  $V_5^0$ , about an order of magnitude smaller. To investigate the role of kinetic energy we explore the dynamics of electrons starting from the 1D Hubbard-Wigner model  $H_{\text{HW}} = H_{\text{Coul}} + H_{\text{kin}}$  [8], where

$$H_{\text{kin}} = \sum_{i,j} t_{ij} (c_{i+1}^\dagger c_i + c_i^\dagger c_{i+1}) \quad (2)$$

describes the hopping of an electron with spin  $\sigma$ . Due to the almost  $90^\circ$  Cu-O-Cu angle the hopping  $t_1$  between nearest neighbor Cu sites results mainly from direct  $d$ - $d$  exchange, while  $t_2$  originates from hopping via a Cu-O-O-Cu path [15] (Fig. 1), leading to the remarkable fact  $|t_2| > |t_1|$ . We adopt here as typical values  $t_1 \approx 63$

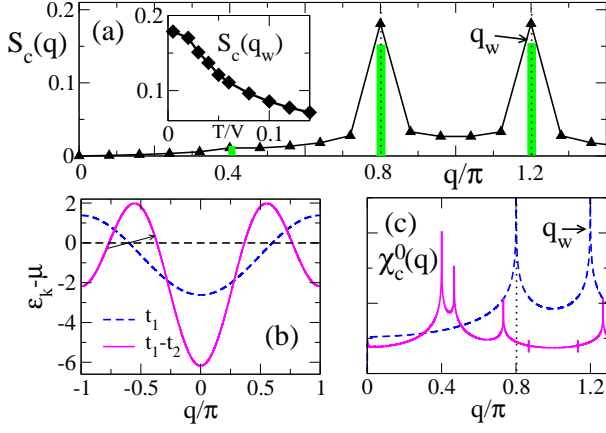


FIG. 3: (color online) (a) Static charge structure factor  $S_c(q)$  calculated for interacting spinless fermions and  $t_1 = 0.04V$ ,  $t_2 = 0.06V$  at  $x = 0.6$  indicates the instability towards WL ordering with modulation  $q_w = 1.2$  (solid line as guide to the eye). Inset shows the temperature dependence of  $S_c(q_w)$ . (b) Comparison of electron dispersions for a system with nearest neighbor hopping  $t_1 (= 1)$  only (dashed line) and for  $t_1 = 1$ ,  $t_2 = 1.5$  (solid line) with the Fermi energy indicated by a horizontal line. (c) While the charge susceptibility  $\chi_c^0(q)$  for noninteracting spinless fermions in the  $t_1$  model shows a logarithmic divergence at  $2k_{SF} = q_w$ , the singularities of the  $t_1$ - $t_2$  model are at different momenta.

meV,  $t_2 = 94$  meV, derived from ab-initio band structure calculations for the  $Cu^{2+}$  edge-sharing reference system  $Li_2CuO_2$  [16]. These values are indeed much smaller than our estimates for  $U = 3.8$  eV and  $V = 1.5$  eV based on optical data for  $Li_2CuO_2$  [15].

Using exact diagonalization we have calculated the static structure factor  $S_c(q)$  for chains up to 25 sites. The peaks of  $S_c(q)$  at  $q_w = 1.2$  (and at  $0.8 = 2 - q_w$ ) are characteristic for a WL modulation at  $x = 3/5$  (Fig. 3(a)). Since the magnetic energy scale is much smaller than the Coulomb interaction  $V$ , the charge structure can be determined by disregarding spin degrees of freedom, namely in terms of spinless fermions (SF). The SF-CDW arises as an instability due to low energy scattering between the two Fermi points at  $k_{SF}$  which lead to a singularity in the charge susceptibility  $\chi_c^0(q)$  at  $q = 2k_{SF} (= 4k_F)$ . Subsequent inclusion of interactions is expected to change the character of a singularity, yet not the momentum at which the singularity occurs. This explains the origin of the  $4k_F$  CDW instability in interacting 1D systems and, as  $4k_F = 2\pi/n$ , the coincidence with the modulation period  $n$  of the WL.

The equivalence of WL and CDW periodicity disappears when  $t_2 > t_1$  ( $= 0.38$  at  $x = 0.6$ ); then there are four instead of two Fermi points leading to new singularities in  $\chi_c^0(q)$  (Fig. 3(b,c)) and to a shift of the original singularity away from  $4k_F = q_w$ . In this case the standard tools of many body theory such as bosonization [11] suggest a change of the modulation period. This, how-

ever, is not reflected in the experiment and is also not observed in our numerical results for  $S_c(q)$  (Fig. 3(a)). In fact, the singularity remains at  $q_w$  up to a value  $t_2 \sim 4t_1$ , a striking manifestation that the structure is robust and controlled by the long range Coulomb interaction [17]. The calculated  $S_c(q)$  shows besides the main peak at  $q_w$  a weak higher harmonic feature at  $q = 2q_w = 2.4$ , consistent with the relative intensities of structural reflexes calculated from the experimentally determined Cu ion positions (vertical bars in Fig. 3(a)). Further results (inset Fig. 3(a)) reveal that WL correlations persist up to temperatures  $k_B T = 0.05V$ , consistent with experiment.

The magnetic susceptibility ( $T$ ) was measured in the temperature range from 5 K to 350 K using a SQUID magnetometer. The data (Fig. 4(a)) reveal strikingly different temperature dependences for the two compounds:

( $T$ ) for  $Na_3Cu_2O_4$  displays some similarity with a nearest neighbor Heisenberg antiferromagnetic chain [18], whereas the  $Na_8Cu_5O_{10}$  data show continuous increase down to low temperature until its maximum near 25 K is reached. Both systems reveal antiferromagnetic correlations, yet magnetic order is observed only for  $Na_8Cu_5O_{10}$  at  $T_N = 23.5$  K. For a calculation of ( $T$ ) we assume that the spins remain fixed at their positions  $R_i$  as given by the structural analysis and by  $H_{HW}$  (Fig. 2). This leads to a generalized Heisenberg model

$$H_{Heis} = \frac{1}{2} \sum_{i,j} J(R_i - R_j) S_i \cdot S_j; \quad (3)$$

where the exchange constants depend on the distance  $|R_i - R_j|$  between the spins and on the direction (parallel to the chains or perpendicular). For  $x = 0.5$  only the exchange constants  $J_2, J_4, \dots$  along the chains contribute, while for  $x = 0.6$   $J_1, J_2, J_3, \dots$  are relevant. Apart from the modulated spin pattern, superexchange [19] in WL's shows further novel features, namely fluctuations (a) of spin positions and (b) of antiferromagnetic exchange integrals  $J_1 = 4t_1^2/(U + V)$  due to the low energy charge fluctuations. The energy shifts ( $V$ ) due to  $V_1$  depend on the WL structure, and are in general different for left (right) scattering processes (see Fig. 2(b)). The exchange constants may be estimated from the parameters specified above. The largest coupling is  $J_2 = 100 - 200$  K resulting from superexchange via a Cu-O-O-Cu path. Because of the almost  $90^\circ$  Cu-O-Cu bond angle (13)  $J_1$  exchange is smaller. Yet in the case of  $J_1$  there are additional exchange contributions, which have to be taken into account. The most important of these involve  $O p^4$  configurations with Hund interaction on oxygen [20], such that the total  $J_1$  may become negative.

We have used finite temperature diagonalization (FTD) [21] to calculate ( $T$ ) for  $Na_3Cu_2O_4$  studying chains up to  $N = 48$  sites (24 spins). Good agreement with experiment was achieved with  $J_2 = 172$ ,  $J_4 = 17$  K and 1.97 for the g-factor. The small antiferromagnetic interchain coupling  $J^0 = 34$  K (Fig. 4(b)) is frustrating as

